X-ray microscopy reveals the outstanding craftsmanship of Siberian Iron Age textile dyers

Andreas Späth[1,*,‡], Markus Meyer[1,‡], Thomas Huthwelker[2], Camelia N. Borca[2], Karl Meßlinger[3], Manfred Bieber[4], Ludmilla L. Barkova[5,†], Rainer H. Fink[1,6,*]

Affiliations:

[1]Physical Chemistry II and Interdisciplinary Center for Molecular Materials, Friedrich Alexander University Erlangen-Nürnberg (FAU), Egerlandstraße 3, 91058 Erlangen, Germany.

[2]Swiss Light Source (SLS), Paul Scherrer Institut, 5232 Villigen, Switzerland.

[3]Physiology and Pathophysiology, Friedrich Alexander University Erlangen-Nürnberg (FAU), Universitätsstraße 17, 91054 Erlangen, Germany.

[4]Ex Oriente, Waldleite 17, 97295 Waldbrunn, Germany.

[5]Department of Eastern European and Siberian Archaeology, The State Hermitage Museum, 38 Dvortsovaya Embankment, 190000 Saint Petersburg, Russia.

[6]Center for Nanoanalysis and Electron Microscopy (CENEM), Friedrich Alexander University Erlangen-Nürnberg (FAU), Egerlandstraße 3, 91058 Erlangen, Germany.

* Correspondence to: andreas.spaeth@fau.de (A.S.); rainer.fink@fau.de (R.H.F.)

‡ These authors contributed equally to this work.

† deceased

Abstract:

The excellent craftsmanship of ancient Oriental and Central Asian textile dyers is already demonstrated in the remarkable brilliance and fastness of the colors of the so-called Pazyryk carpet, the by far oldest pile carpet found to date. We employed μ-XRF imaging to detect the distribution of metal organic pigments within individual fibers of the Pazyryk carpet and to compare the results with wool fibers, which we have prepared according to a traditional Anatolian dyeing recipe that includes fermentation of the wool prior to dyeing. We observe congruent pigment distribution in several specimens and conclude that the superior fermentation technique has been utilized about 2,000 years earlier than it has been known so far.

One Sentence Summary:

μ-XRF detects characteristic pigment distributions along cross-sections of Oriental carpet wool fibers to disclose ancient dyeing procedures.

Main Text:

Since centuries many people all over the world are fascinated by the brilliance and persistence of colors in traditional oriental carpets and flat weaves. Since natural dyes often consist of a mixture of various colorants, the resulting colors have a more vivid color depth than synthetic dyes *(1,2)*. Many natural colorants require a mordant (typically a transition metal salt, e.g., $KAlSO_4$, $FeSO_4$, etc.) to form a metal-organic complex pigment *(3-5)*. Mordants typically increase the fastness of a dye by enhanced binding to the wool tissue, but can also influence the hue of the color.

X-ray fluorescence microscopy (μ-XRF) is a suitable technique for high-resolution imaging of metal based pigments. Its outstanding capabilities in terms of spatial resolution and elemental sensitivity have been demonstrated for the analysis of pigments in cultural heritage samples, such as masterpiece paintings *(6-8)*, handwritings *(9,10)*, metal artefacts *(11,12)* and other solid objects *(13)*. Here, we present the first study employing high-resolution μ-XRF for the *in-situ* analysis of pigments within a textile sample with high historical relevance.

An outstanding example for the art of ancient natural dyeing is the Pazyryk carpet – a sheep wool pile carpet with a size of 1.83 x 2 m² consisting of ~ 360,000 Turkish knots found in a Saka kurgan tomb from the 4^{th} – 3^{rd} century B.C in the Altai mountains (Fig. S1) *(14,15)*. The carpet was well preserved by a permafrost ice lens until its discovery by Russian archaeologists in 1947 and still shows vivid red and yellow colors. It is so far the oldest known pile carpet – exceeding the next dated specimens by at least six centuries – and exhibits a mature craftsmanship that suggests several human generations of experience in production of such textiles *(14)*. Therefore, the Pazyryk carpet is a unique representative of ancient Central Asian cultural heritage.

Considering the excellent color fastness it is of interest to understand the dyeing procedure used by the Pazyryk culture. Since the 1970s cultural anthropologists have studied and revived traditional Anatolian dyeing techniques based on fermentation of wool prior to dyeing *(16,17)*. They described a remarkable improvement of color fastness against bleaching that is superior to textiles from industrial production for various natural colorants. Nevertheless, the fermentation technique had been almost forgotten at the time of these studies, because of its comparably slow production cycle (three weeks for the fermentation procedure) and the risk of putrefaction when performed poorly *(17)*.

Fig. 1 depicts the morphological components of individual wool fibers and the influence of fermentation as confirmed by scanning electron microscopy (SEM) *(18,19)*. Fermentation with *G.*

candidum yeast leads to an abduction of the outermost layers of the cuticle by consumption of the fatty interstices in-between the cuticle scales. Furthermore, *G. candidum* stabilizes the pH inside the hair to 4.4 resulting in saturation of naturally deprotonated thiol groups (R-S-H) within the cuticle. Both effects increase the permeability of the cuticle for metal-organic compounds *(20,21)*. Diffusion of metal-organic colorants inside the wool fiber takes places mainly inside the cell-membrane-complex (CMC) *(20)*. The CMC is a network of fatty acid layers that glues the keratin based components (cortex cells and cuticle scales) together *(22)*.

It is proposed that the increased color fastness of fermented sheep wool stems from a deeper and also overall higher amount of uptake of pigments inside the fibers. In natural hair, the cuticle forms a moderate barrier between CMC and infiltrating metal-organic mordant dyes. After fermentation this diffusion channel is easier accessible and the dye is more likely to accumulate deep inside the fiber cortex causing a more intense and stable coloring. In transmission electron microscopy (TEM) images of cross-sections from fermented and dyed wool fibers the CMC appears darker than the surrounding cortex, which is not the case in not fermented, but identically dyed analogues (Fig. S2). We also see this effect in TEM micrographs of the Pazyryk carpet. However, this is no clear evidence of the presence of the pigment inside the CMC, since TEM does not provide sufficient chemical information. In principle SEM imaging can prove the fermentation process directly by detection of off-standing cuticle cells. However, this is usually only possible for recent or rarely used textiles, since long-term use leads to a loss of the outer cuticle layers by abrasion (Fig. S3) *(17)*.

We have prepared freshly sheared wool from Anatolian sheep according to traditional dyeing procedures as passed on in Eastern Anatolia since generations *(16,17)*. All specimens were dyed with madder (*R. tinctorum*) and $KAl(SO_4)_2$, because the resulting pigment Turkey red is one of the most common red natural colorants in Middle East since centuries *(2)*. The use of *R. tictorum* by the Pazyryk culture has been shown by chromatography and UV/Vis spectroscopy *(23)* of extracted pigment. The fibers were embedded in epoxy and cross-sections were prepared by microtome sectioning. We have also used scanning transmission X-ray microscopy (STXM) to verify that the morphology (also in terms of chemical composition) of the ancient fibers were not altered by age, which might have caused an a posteriori migration of pigments within the fibers (cf. Fig. S4).

Fig. 2 shows μ-XRF maps of several individual wool fibers from various specimens. The Al distribution along the cross-section of the recently dyed fibers is compared to samples from the Pazyryk carpet and an 18th century carpet from Turkey as well as natural wool fibers from the same batch as the recently dyed specimens. For the recently fermented wool (Fig. 2A) we detect a deep penetration of a significant amount of aluminum into the fiber cortex with a strong gradient from the cuticle towards the center of the fiber, while the not fermented analogue (Fig. 2D) shows aluminum just within the outer part of the cuticle, although the dyeing procedure was the same in both cases. The undyed natural wool fiber (Fig. 2E) shows only minor contamination on the surface of the fiber as to expect for a sample from a natural source. The Pazyryk carpet and the Konya carpet show a very similar characteristic in their aluminum distribution with a gradient from the cuticle towards the fiber center, but still a significant amount of aluminum deep inside the cortex. For maps of the wool fibers themselves, cf. Fig. S5 (S *K*-edge maps).

We recorded μ-XRF maps of several individual wool fibers for all specimens. The averaged and normalized fluorescence intensities are depicted in Fig. 3. In all cases we compare also the outer part of the fiber (mainly cuticle) with the inner part (mainly cortex). While the natural wool sample shows almost no aluminum (in the cuticle it is even less than in the embedding epoxy used as reference for normalization), the not fermented, but dyed fibers took up the pigment to some extend into the cuticle, but not into the cortex. All other samples show a gradient of aluminum towards the fiber center. However, the overall amount of pigment is much higher in the fermented sample and moreover, a significant uptake within the inner cortex is detected. The variations in the absolute amounts of aluminum uptake for the recently fermented and the ancient specimens might be caused by leaching, but of course the initial concentrations of the dyeing solutions are unknown for the Konya and Pazyryk fibers.

We conclude from our studies that both the 18th century Konya carpet and the Pazyryk carpet have been manufactured from wool that was fermented prior to dyeing. This means that the people of the Pazyryk culture not only already had sophisticated knowledge about pile carpets, but were also highly skillful textile dyers achieving color fastness superior to modern industrial production. Our results also proof that the fermentation technique was in ancient times not only restricted to Eastern Anatolia and may have played an important role in traditional dyeing craftsmanship. Furthermore, we have demonstrated the high potential of μ-XRF imaging in analysis of textile cultural heritage and see great potential for further high-resolution *in-situ* studies in this field. In the best case our

results might motivate contemporary textile dyers to learn from ancient craftsmanship and develop an efficient fermentation based dyeing recipe.

References and Notes:

1. J. N. Liles, *The Art and Craft of Natural Dyeing* (The University of Tennessee Press, Knoxville, 1990).
2. T. Bechtold, R. Mussak, *Handbook of Natural Colorants* (John Wiley & Sons, Chichester, 2009).
3. P. S. Vankar, *Chemistry of Natural Dyes*. Resonance **5(10)**, 73-80 (2000).
4. E. S. B. Ferreira, A. N. Hulme, H. McNab, Anita Quye, *The natural constituents of historical textile dyes*. Chem. Soc. Rev. **33**, 329-336 (2004).
5. M. Zarkogianni, E. Mikropoulou, E. Varella, E. Tsatsaroni, *Colour and fastness of natural dyes: revival of traditional dyeing techniques*. Color. Technol. **127(1)**, 18-27 (2011).
6. J. Dik, K. Janssens, G. van der Snickt, L. van der Loeff, K. Rickers, M. Cotte, *Visualization of a Lost Painting by Vincent van Gogh Using Synchrotron Radiation Based X-ray Fluorescence Elemental Mapping*. Anal. Chem. **80(16)**, 6436-6442 (2008).
7. K. Janssens, J. Dik, M. Cotte, J. Susini, *Photon-Based Techniques for Nondestructive Subsurface Analysis of Painted Cultural Heritage Artifacts*. Acc. Chem. Res. **43(6)**, 814-825 (2010).
8. M. Ahlfeld, L. de Viguerie, *Recent developments in spectroscopic imaging techniques for historical paintings - A review*. Spectrochim. Acta B **136**, 81-105 (2017).
9. O. Hahn, W. Malzer, B. Kanngiesser, B. Beckhoff, *Characterization of iron-gall inks in historical manuscripts and music compositions using x-ray fluorescence spectrometry*. X-Ray Spectrom. **33**, 234-239 (2004).
10. J. Duh, D. Krstić, V. Desnica, S. Fazinić, *Non-destructive study of iron gall inks in manuscripts*. Nucl. Instrum. Meth. B. **417**, 96-99 (2018).
11. B. Constantinescu, A. Vasilescu, M. Radtke, U. Reinholz, *A study on gold and copper provenance for Romanian prehistoric objects using micro-SR XRF*. J. Anal. At. Spectrom. **26**, 917-921 (2011).
12. D. Grolimund, D. Berger, S. Bolliger Schreyer, C. N. Borca, S. Hartmann, F. Müller, J. Hovind, K. Hunger, E. H. Lehmann, P. Vontobel, H. A. O. Wang, *Combined neutron and synchrotron X-*

ray microprobe analysis: attempt to disclose 3600 years-old secrets of a unique bronze age metal artifact. **26**, 1012-1023 (2011).

13. K. Janssens, G. Vittiglio, I. Deraedt, A. Aerts, B. Vekemans, L. Vincze, F. Wei, I. Deryck, O. Schalm, F. Adams, A. Rindby, A. Knöchel, A. Simionovici, A. Snigirev, *Use of Microscopic XRF for Non-destructive Analysis in Art and Archaeometry*. X-Ray Spectrom. **29**, 73-91 (2000).
14. S. I. Rudenko, *Frozen tombs of Siberia: The Pazyryk Burials of Iron-Age Horsemen* (University of California Press, Berkeley, 1970).
15. K. S. Rubinson, *The textiles from Pazyryk*. Expedition **32**, 49-61 (1990).
16. V. G. Moschkova, *Die Teppiche der Völker Mittelasiens im späten XIX. und frühen XX. Jahrhundert* (FAN, Tashkent, 1970).
17. M. Bieber, „Das Kavacık-Projek“ in *Anatolische Dorfteppiche* (Niederrheinisches Museum für Volkskunde und Kulturgeschichte, Kevelaer, 1988), pp. 37-55.
18. K. Meßlinger, „Elektronenmikroskopische Überprüfung alter Färbeverfahren“ in *Anatolische Dorfteppiche* (Niederrheinisches Museum für Volkskunde und Kulturgeschichte, Kevelaer, 1988), pp. 55-57.
19. M. Meyer, C. N. Borca, T. Huthwelker, M. Bieber, K. Meßlinger, R. H. Fink, A. Späth, *μ-XRF Studies on the Colour Brilliance in Ancient Wool Carpets*. Scanning **2017**, 6346212 (2017).
20. F.-J. Wortmann, G. Wortmann, H. Zahn, *Pathways for Dye Diffusion in Wool Fibers*. Text. Res. J. **67(10)**, 720-724 (1997).
21. G. Freddi, T. Arai, G. M. Colonna, A. Boschi, M. Tsukada, *Binding of Metal Cations to Chemically Modified Wool and Antimicrobial Properties of the Wool–Metal Complexes*. J. Appl. Polym. Sci. **82(14)**, 3513-3519 (2001).
22. C. R. Robbins, *Chemical and Physical behavior of Human Hair* (Springer, Berlin/Heidelberg, ed. 5, 2012).
23. G. G. Balakina, V. G. Vasiliev, E. V. Karpova, V. I. Mamatyuk, *HPLC and molecular spectroscopic investigations of the red dye obtained from an ancient Pazyryk textile*. Dyes Pigments **71**, 54-60 (2006).
24. A. Späth, M. Meyer, S. Semmler, R. H. Fink, *Microspectroscopic soft X-ray analysis of keratin based biofibers*. Micron, **70**, 34-40 (2015).

25. J. Raabe, G. Tzvetkov, U. Flechsig, M. Böge, A. Jaggi, B. Sarafimov, M. G. C. Vernooij, T. Huthwelker, H. Ade, D. Kilcoyne, T. Tyliszczak, R. H. Fink, C. Quitmann, *PolLux: A new facility for soft x-ray spectromicroscopy at the Swiss Light Source*. Rev. Sci. Instrum. **79**, 113704 (2008).

26. B. L. Henke, E. M. Gullikson, *X-Ray Interactions: Photoabsorption, Scattering, Transmission, and Reflection at E = 50-30,000 eV, Z = 1-92*. J.C. Davis, At. Data Nucl. Data, **54**, 181-342 (1993).

27. V. A. Solé, E. Papillon, M. Cotte, P. Walter, J. Susini, *A multiplatform code for the analysis of energy-dispersive X-ray fluorescence spectra*. Spectrochim. Acta B, **62**, 63-68 (2007).

28. B. Patkowska-Sokoła, Z. Dobrzanski, K. Osman, R. Bodkowski and K. Zygadlika, *The content of chosen chemical elements in wool of sheep of different origins and breeds*. Arch. Tierzucht, **52** 410-418 (2009).

Acknowledgments: The authors gratefully acknowledge experimental support by Mrs. Hilde Merkert (University of Würzburg; SEM imaging) and Christoffer Jordan (FAU; TEM sample preparation). A.S. and M.M. acknowledge support by the Graduate School Molecular Science (GSMS). M.M. acknowledges funding by GRK 1896 “In situ Microscopy with Electrons, X-rays and Scanning Probes”. R.H.F. acknowledges support by the German Minister of Education and Research (BMBF), contract 05 K16WED. Travel support was obtained from the European Community’s H2020 framework program (grant agreement 654360, nanoscience foundries and fine analysis, NFFA). We acknowledge beamtime provided at the PHOENIX and PolLux beamlines of the Swiss Light Source (SLS) at the Paul Scherrer Institut, Villigen, Switzerland.

Author contributions: M.B. prepared and provided the recent wool specimens and the sample from the Konya carpet. A.S., R.H.F., L.L.B. and K.M. planned the experimental analysis. M.M and K.M. performed the electron microscopy experiments and M.M, K.M. and L.L.B. analyzed the respective data. A.S., M.M., T.H. and C.N.B. conducted μ-XRF experiments at the PHOENIX beamline. A.S. recorded and analyzed STXM micrographs at the PolLux beamline. M.M. and A.S. evaluated the μ-XRF data. A.S. wrote the manuscript and M.M., T.H., C.N.B., K.M., M.B. and R.H.F. revised it.

Competing interests: The authors declare no competing interest.

Data and materials availability: All data are available from the corresponding authors upon request in original as well as in processed form.

Supplementary Materials:

Materials and Methods

Figures S1-S7

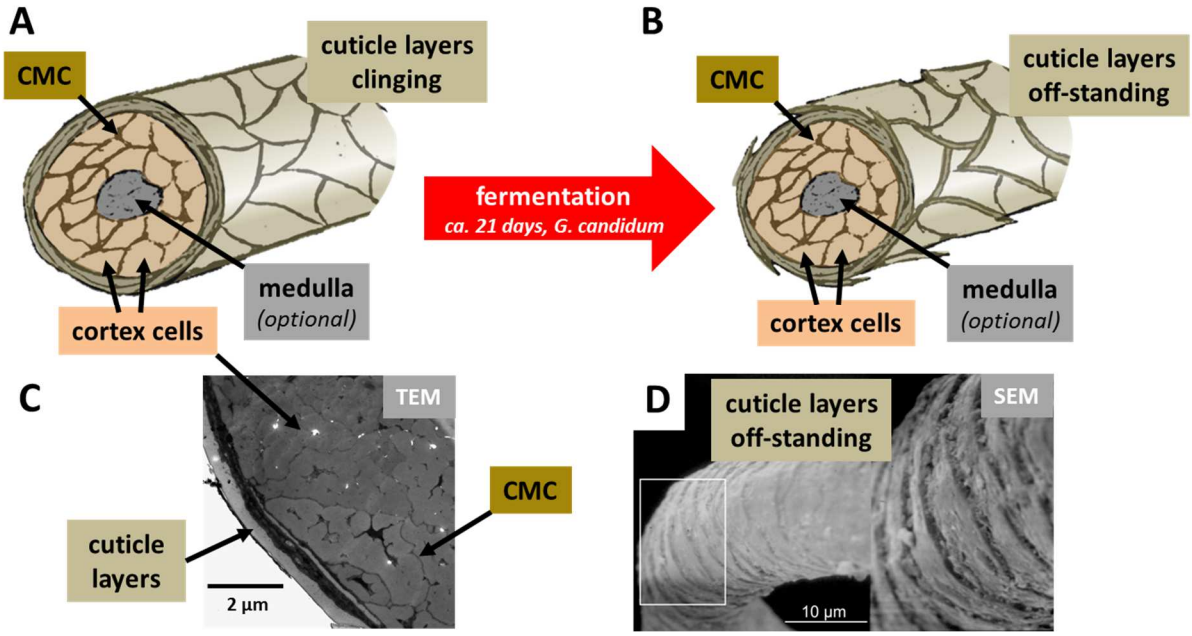

Fig. 1. Scheme depicting the effects of fermentation on wool fibers. A) Natural wool fiber depicting cortex cells, CMC and surrounding cuticle layers. The medulla is a porous structure inside thicker wool fibers that is rarely found in Anatolian sheep shearings as used for carpet production. B) After 3 weeks fermentation with *G. candidum*, the cuticle layers are protruding

from the fiber. C) TEM image depicting cortex, CMC and cuticle layers in a cross-section of Anatolian sheep wool. D) SEM image of off-standing cuticle layers after fermentation.

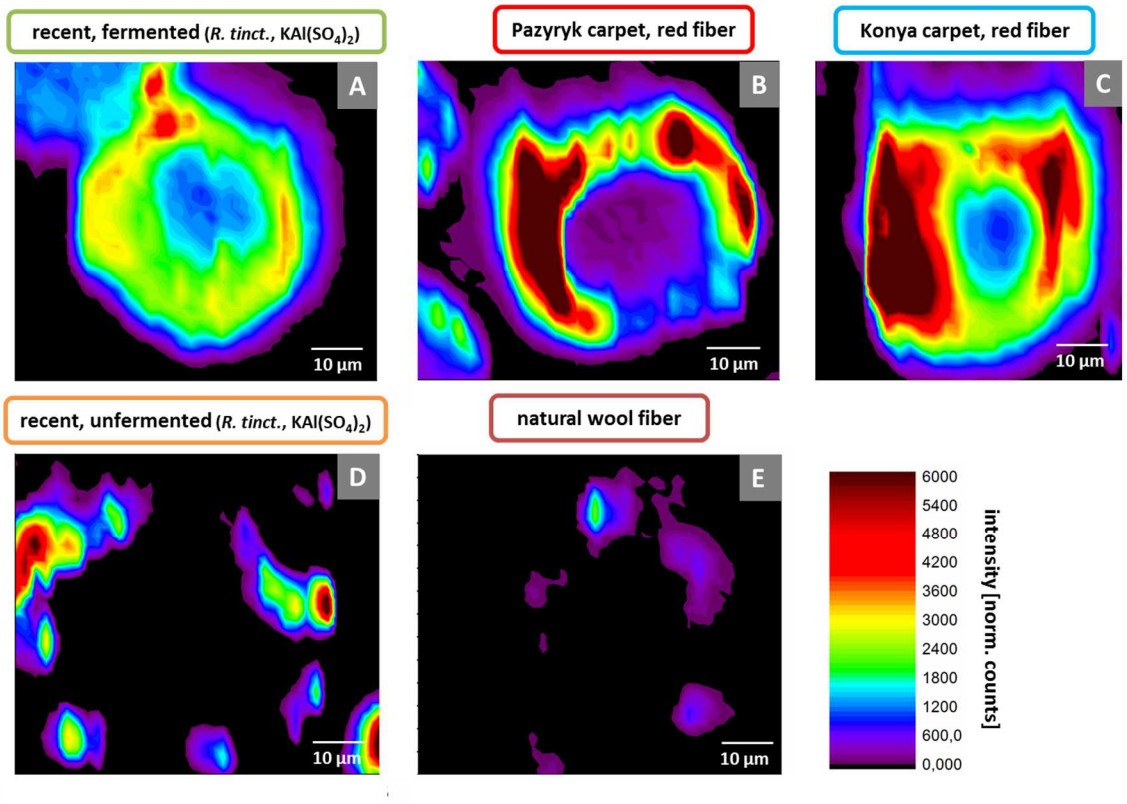

Fig. 2. μ-XRF maps (Al *K*-edge; pixel size 2x2 µm²) of various sheep wool specimens. A) Recently fermented and dyed with *R. tinctorum* / $KAl(SO_4)_2$. B) Red fiber from Pazyryk carpet. C) Red fiber from a carpet from the 18th century (origin: Konya, Turkey). D) Recently dyed with *R. tinctorum* / $KAl(SO_4)_2$, no fermentation. E) Natural wool fiber. The maps provide an *in-situ* visualization of

the pigment distribution within the wool fibers. They show an increased uptake of Al especially into the inner regions of the wool fibers when fermentation has been applied prior to dyeing.

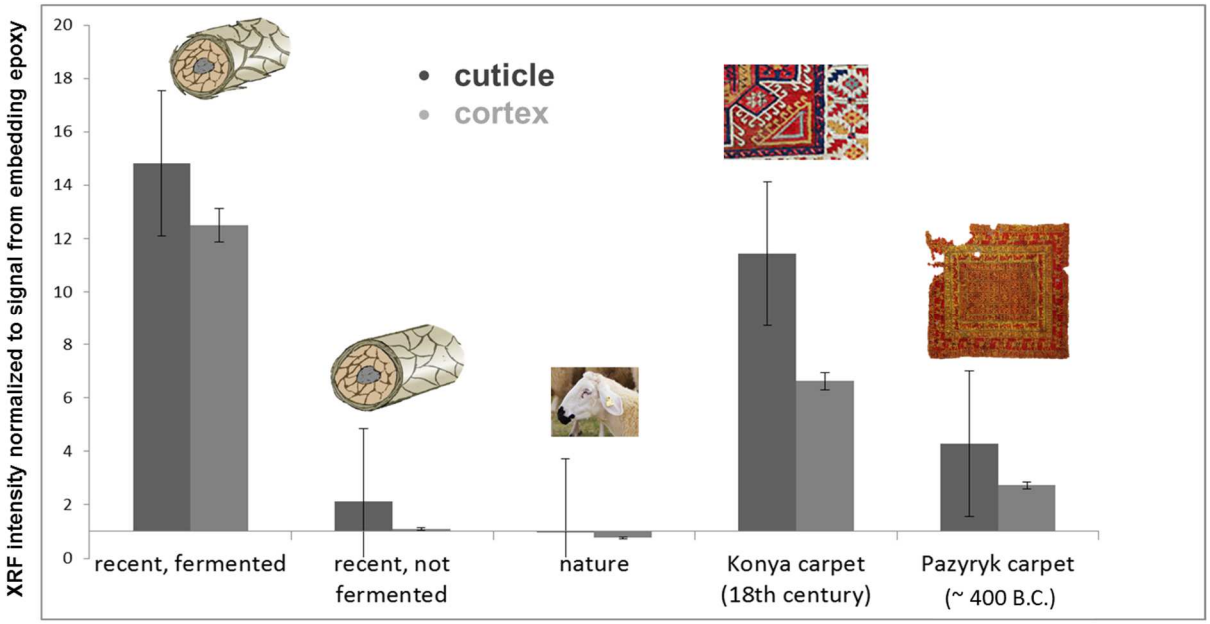

Fig. 3. Normalized Al *K*-edge intensities equivalent to pigment uptake for various wool specimens with respect to depth of penetration (average over 5 – 8 individual fibers). Normalization was conducted with respect to the embedding epoxy. Therefore, it was possible to correct for geometric effects from varying sample dimensions (cf. Fig. S6). A strong enhancement of the Al concentration especially in the cortex of the fibers of the Konya and Pazyryk carpet wool is attributed to fermentation prior to dyeing. Averaging over several fibers of each batch minimizes variances from asymmetric embedding or local density variations within individual fibers that are given by nature.

Supplementary Materials for

X-ray microscopy reveals the outstanding craftsmanship of Siberian Iron Age textile dyers

Andreas Späth*,‡, Markus Meyer‡, Thomas Huthwelker, Camelia N. Borca, Karl Meßlinger, Manfred Bieber, Ludmilla L. Barkova†, Rainer H. Fink*

* Correspondence to: andreas.spaeth@fau.de; rainer.fink@fau.de
‡ These authors contributed equally to this work.
† deceased

This PDF file includes:

Materials and Methods

Sample preparation

The recently prepared wool was obtained from traditional Anatolian fat-tailed sheep (*Ak Karaman*). The process of dyeing for the recently prepared wool fibers is described in more detail in *(17)*. The fermentation process is started with a suspension of sourdough and wheat bran. The latter fosters selective growth of *G. candidum* yeast due to a high content of pentosan. The *G. candidum* culture regulates the pH to 4.4 and hinders the growth of putrefactive bacteria. Within about three weeks of fermentation *G. candidum* decomposes lipids inside the cuticle layers of the wool enhancing permeability within the subsequent dyeing process. After fermentation madder roots and mordant are added to the suspension at ambient conditions. Red fibers are obtained with $KAl(SO_4)_2$ mordant (20 vol.-% solution). The unfermented specimens have been dyed under identical conditions without previous fermentation.

The specimen from the Pazyryk carpet has been extracted by the former curator Ludmilla Barkova from a loose part of the carpet designated for scientific studies. The specimen from the Konya carpet (Museum for Islamic Art, Berlin) has been extracted by Manfred Bieber. Both specimens have been kept under clean and dark conditions until embedding.

The various specimens were embedded in an epoxy resin derived from a 1:1 mixture of 4,4'-Methylenebis(2-methylcyclohexylamine) and Trimethylolpropane triglycidyl ether. This epoxy provides very good contrast in X-ray microscopy of biological samples at the C *K*-edge *(24)*. After drying for three days at room temperature, the sample blocks were trimmed to pyramidal shape and microtomed with a diamond knife to obtain a flat surface along the cross section of several isolated wool fibers (Fig. S6) for μ-XRF mapping. This sample preparation procedure was used, since previous μ-XRF mapping on thin sections of various thicknesses (200 nm – 3 µm) was not successful. The overall amount of Al within the corresponding small sample volumes of these thin sections was below the detection limit of the method.

Thin sections (~ 200 nm) gained during microtoming of the sample blocks were transferred to TEM grids and used for STXM imaging.

Samples for TEM imaging have been embedded in EpoFix (Struers GmbH). After drying over night at room temperature the hardened material was trimmed and microtomed to ~ 100 nm thin cross sections.

TEM imaging

TEM imaging was performed with a Zeiss LEO 912 Omega (Physical Chemistry II, FAU) operated at 80 kV and in low magnification mode.

STXM imaging

STXM measurements where performed at the PolLux beamline at the Swiss Light Source in Villigen, Switzerland *(24)*. The micrographs were recorded at the C *K*-edge resonance of keratin (288.1 eV) *(25)* with a 25 nm Ni Fresnel zone plate, a pixel size of 25x25 nm² and a dwell time of 10 ms per pixel.

μ-XRF imaging

μ-XRF studies were performed at the PHOENIX beamline at the Swiss Light Source. The X-ray beam was focused to 3 x 5 μm^2 and the pixel size was 2 x 2 μm^2. The excitation energy for fluorescence mapping was 2.05 keV and the dwell per pixel was 2 s. The samples were mounted under 45° degree relative to the incoming beam to allow penetration of X-rays into the sample and an exit of the elemental fluorescence signals from the specimen. Fluorescence maps were recorded by scanning the sample relative to the fixed position of the microbeam. The energy dispersive X-ray fluorescence spectra were recorded for each position using a single-element solid state detector (Ketek) with 160 eV energy resolution. For the best quality of the Al K_α emission line in the fluorescence spectra in terms of signal to noise ratio and intensity, the excitation energy was chosen at 2.05 keV, as close as possible to the Al *K* edge. However, at this photon energy the sulfur emission line (for proper fiber localization) cannot be recorded, as the S *K*-edge (2.47 keV *(26)*) is above the energy of the incoming photons. Therefore, the higher order suppression of the beamline was deactivated, resulting in a small portion of third order light from the monochromator (6.15 keV). We calculated the contribution of the third order light by measuring a $KAl(SO_4)_2$ standard (3.0 mg in 100 mg cellulose). This allowed calculating the portion of higher order light to be ~ 2%, while 98% was first order light. This low portion was sufficient to record S *K*-edge maps, but will not significantly affect the Al *K*-edge maps.

Data evaluation

STXM maps have been analyzed with aXis2000.

Fluorescence maps have been fitted and analyzed with PyMca *(27)*. An exemplary fit is depicted in Fig S7. The attenuation of the excitation and fluorescence photons within the hair fibers was calculated based on literature values for the mean elemental distribution of chemical elements in sheep wool *(22, 28)*, the mean density of wool fibers (1.4 g/cm^3) *(22)* and respective attenuation factors *(26)*. With this method we could calculate the energy dependent probing depth (~ 20 μm at 2.05 keV, ~ 360 μm at 6.15 keV) and correlate the fluorescence signals to the qualitative metal contents. An exact quantitative evaluation of the Al content within the specimens would not be legitimate, since the density of the wool fibers is by nature not exactly determined. Therefore, we restricted our analysis to qualitative measures that are reliable for each individual fiber. We have estimated that the mean Al content within the cuticle of fermented fibers (highest measured intensities) is in the order of 0.1 %.

For comparison of the Al *K*-edge fluorescence intensities of different specimens, the intensities have been normalized to the Al signal from the embedding epoxy. The epoxy should have a constant distribution of Al traces (confirmed by constant intensity in Al *K* edge emission). This method allows for a proper treatment of geometrical variances of the epoxy stubs leading to slightly varying incidence angle for each sample.

Fig. S1.

Photograph of the Pazyryk carpet in the exhibition of The State Hermitage Museum, St. Petersburg. The fibers for the present analysis have been extracted from a loose piece of the carpet belonging to a missing part in the upper left edge of the photograph that is stored by the museum for scientific purposes.

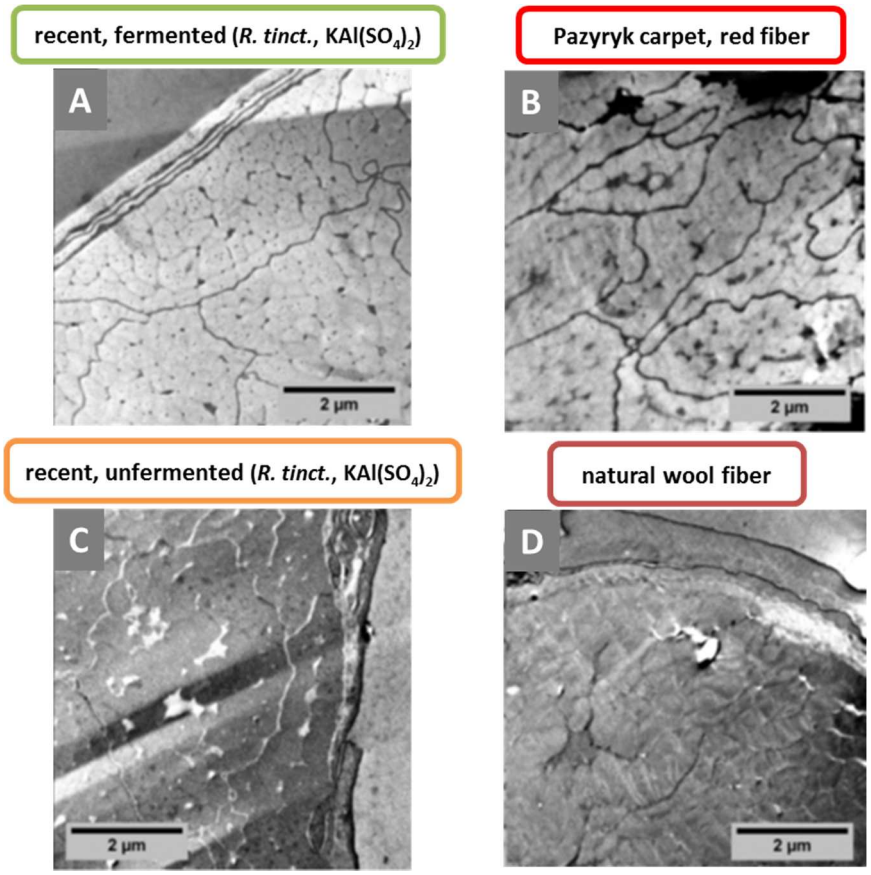

Fig. S2.

TEM micrographs of sheep wool (magnification: 4,000). A) Recently fermented and dyed with madder roots and $KAl(SO_4)_2$. B) Pazyryk carpet. C) Recently dyed with madder roots and $KAl(SO_4)_2$, no fermentation. D) Natural wool. A) and B) show a darker contrast for the CMC compared to the cortex, while the same structure appears brighter in C). In B), however, the CMC has poor contrast to the cortex. Since diffusion inside the wool fibers is mainly happening within the CMC, these differences in the contrast may be a hint on various amounts of pigment uptake or morphological changes during the fermentation process. However, without further chemical information as provided by μ-XRF imaging, this interpretation stays speculative.

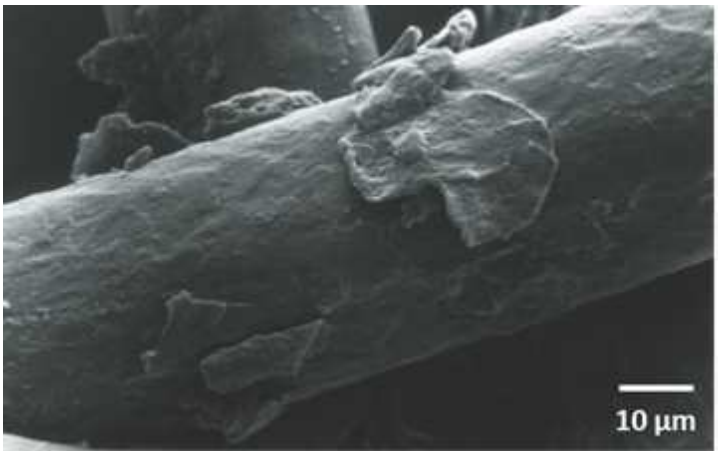

Fig. S3.

SEM micrograph depicting a sheep wool fiber from a Turkish carpet from the 18th century. The outermost cuticle scales are mainly lost by abrasion due to long-term use of the textile *(17, 19)*. This finding is typical for ancient textiles unless they have been preserved very well. Therefore, the direct observation of scale abduction by fermentation of the wool prior to dyeing is usually not possible for ancient or intensely used specimens.

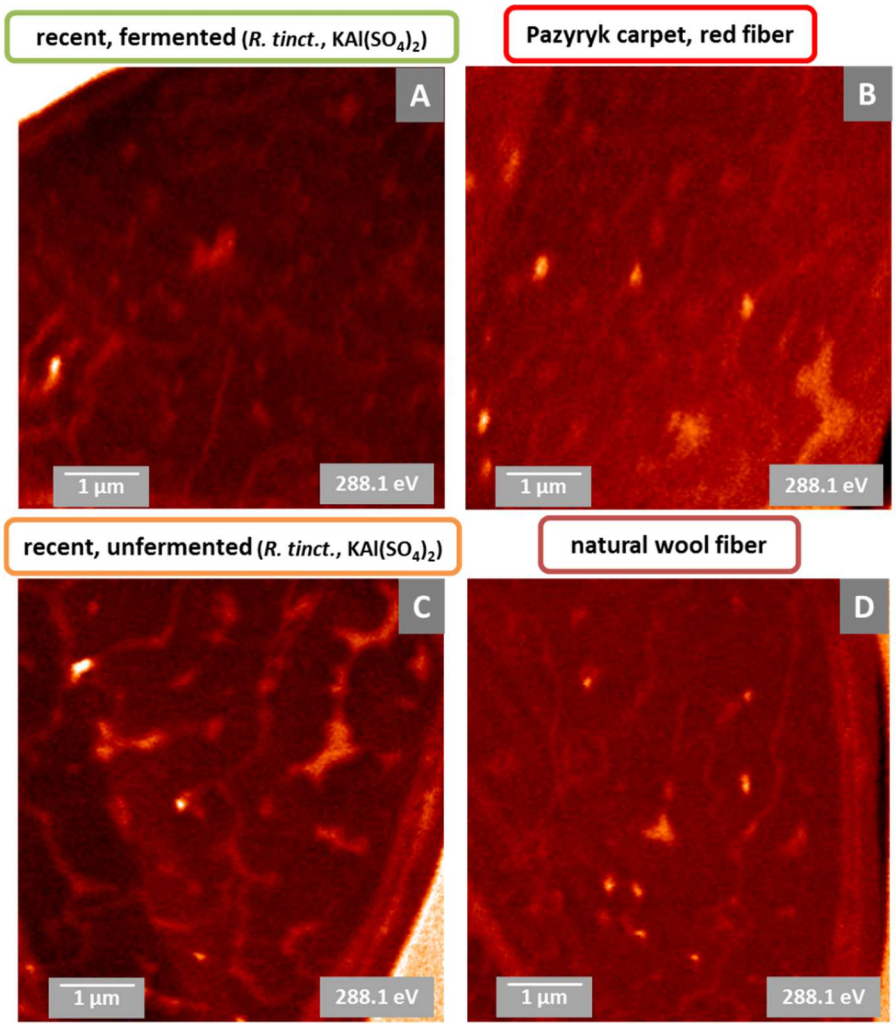

Fig. S4.

STXM micrographs at C *K*-edge resonance of keratin showing optimum contrast for keratinous material (cuticle, cortex) vs. CMC *(25)*. A) Recently fermented and dyed with madder roots and $KAl(SO_4)_2$. B) Pazyryk carpet. C) Recently dyed with madder roots and $KAl(SO_4)_2$, no fermentation. D) Natural wool. The STXM images confirm that the morphology of the wool fibers is still intact after fermentation and that this is also true for the Pazyryk fibers despite their long-term burial. STXM is in that sense more sensitive to chemical composition than TEM.

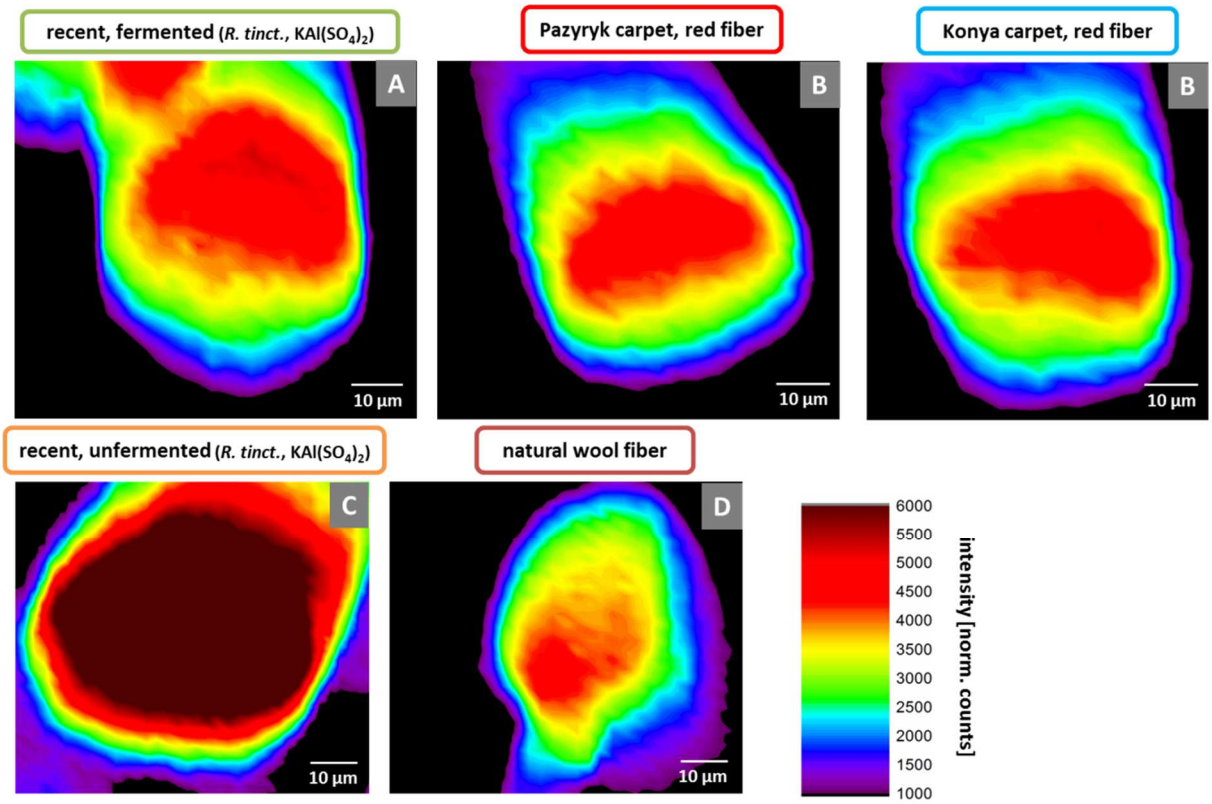

Fig. S5.

μ-XRF maps (S *K*-edge; pixel size 2x2 µm²) of various sheep wool specimens. A) Recently fermented and dyed with *R. tinctorum* / $KAl(SO_4)_2$. B) Red fiber from Pazyryk carpet. C) Red fiber from a carpet from the 18th century (origin: Konya, Turkey). D) Recently dyed with *R. tinctorum* / $KAl(SO_4)_2$, no fermentation. E) Natural wool fiber. The S maps help to define the position the wool fibers, especially for specimens with overall low aluminum uptake. Due to a higher penetration depth, the fibers might, however, appear more asymmetric, since we see more of the continuation of the fibers within the epoxy block and the fibers have a low probability to be embedded straight in-line with the surface normal of the prepared cross section.

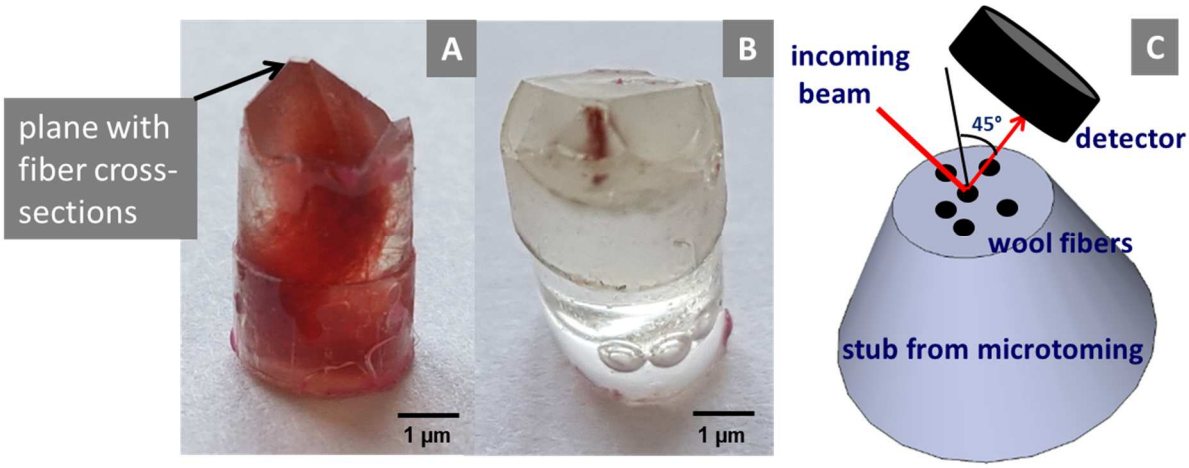

Fig. S6.

Preparation of samples for μ-XRF mapping. A) Recently dyed and fermented wool in epoxy. B) Pazyryk sample. C) Instead of measuring thin sections, the microtome was used to prepare proper cross sections of the wool fibers within the epoxy stub. These stubs were placed in the focus of the X-ray beam under 45° according to the optical axis of the beam as well as the detector.

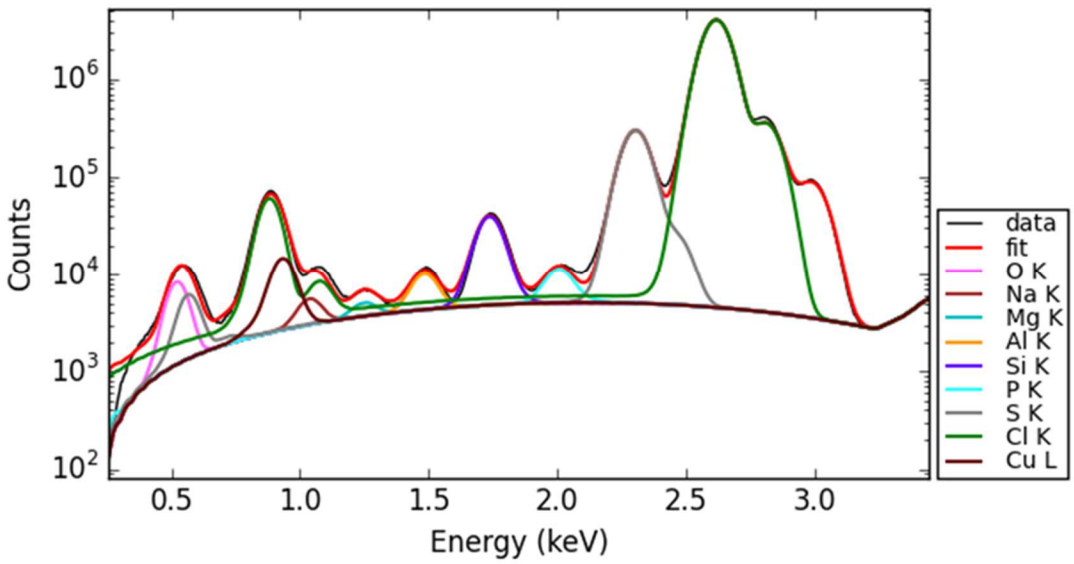

Fig. S7.

Fit for the fluorescence emission spectrum derived by summation over an exemplary 2D μ-XRF map. The high contribution of Cl stems from the embedding epoxy. The depicted peak fitting is the basis for the setting of valid photon energy borders during visualization of 2D elemental distribution maps (e.g., Al or S *K*-edge).